ELSEVIER

Journal of Organometallic Chemistry 493 (1995) 83–89

Journal of Organometallic Chemistry

Synthetic, structural and reactivity studies with new Group 4 transition-metal silyl complexes

Toru Imori [a], Richard H. Heyn [a], T. Don Tilley [a,*], Arnold L. Rheingold [b]

[a] *Department of Chemistry 0506, University of California at San Diego, La Jolla, CA 92093, USA*
[b] *Department of Chemistry and Biochemistry, University of Delaware, Newark, DE 19716-2522, USA*

Received 14 September 1994; in revised form 11 November 1994

Abstract

The silyl chloride complexes $(\eta^5\text{-}C_5H_4SiMe_3)_2Zr[Si(SiMe_3)_3]Cl$ (**1**) and $Cp_2M[Si(SnMe_3)_3]Cl$ (M = Ti (**2**); Zr (**3**); Hf (**4**)) were prepared by reaction of the appropriate metallocene dichloride with a silyl lithium reagent. The X-ray crystal structures of **1** and **3** are described. Methylation of **1**, **3**, and **4** with Grignard reagents afforded $(\eta^5\text{-}C_5H_4SiMe_3)_2Zr[Si(SiMe_3)_3]Me$ (**5**) and $Cp_2M[Si(SnMe_3)_3]Me$ (M = Zr (**6**); Hf (**7**)). Complex **1** is a catalyst for the dehydropolymerization of both $PhSiH_3$ and $^nBu_2SnH_2$ to relatively low molecular weight polymers. Whereas **3** and **4** do not react with carbon monoxide, **2** undergoes CO-induced reductive elimination to $Cp_2Ti(CO)_2$ and $ClSi(SnMe_3)_3$.

Keywords: Silyl; Early transition metals; Polysilane; Zirconium; Stannyl; Carbonylation

1. Introduction

Early transition-metal (d^0) silyl complexes have provided an impressive array of new and unprecedented chemical transformations, both stoichiometric and catalytic [1]. For many of these processes, but most notably for carbon monoxide insertions into M–Si bonds [2–4] and dehydropolymerizations of hydrosilanes [5–7], it has been found that rather subtle changes in substituents at the transition metal or silicon can play a large role in influencing the rate and the course of reaction. Here we report new Group 4 metallocene silyl complexes, based on a variation in the ligand set for zirconium, and on the silyl group–$Si(SnMe_3)_3$. Complexes of the latter type are the second examples of transition metal complexes containing this silyl ligand [8].

2. Synthesis of new silyl complexes

The synthesis of compound **1**, $(\eta^5\text{-}C_5H_4SiMe_3)_2Zr[Si(SiMe_3)_3]Cl$, is analogous to earlier reported preparations of related zirconocene–$Si(SiMe_3)_3$ derivatives [2,3]. The appropriate zirconocene dichloride was combined with the lithium silyl reagent in diethyl ether solvent, and the resulting product was obtained as red needles from pentane (Eq. 1).

This substitution pattern at zirconium gives rise to four separate resonances in the ^1H NMR spectrum for the C_5H_4 hydrogen atoms (δ 5.00, 5.80, 6.76, 7.67; benzene-d_6), which cover a wide range of chemical shift values. For comparison, the two ^1H NMR resonances for the C_5H_4 hydrogens in $(\eta^5\text{-}C_5H_4\text{-}SiMe_3)_2ZrCl_2$ [9] appear at δ 5.93 and δ 6.38 (in benzene-d_6).

Tris(trimethylstannyl)silyl complexes of titanium, zirconium, and hafnium were prepared by silylation of the metallocene dichlorides with $(THF)_3LiSi(SnMe_3)_3$ [8] (Eq. 2). Better yields of the products are obtained when the reactions are initiated at low temperature. This

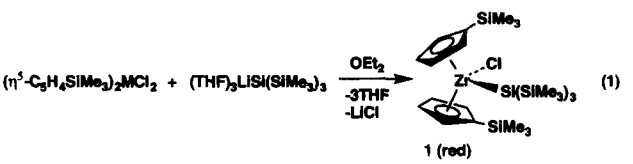

* Corresponding author. Current address: Department of Chemistry, University of California at Berkeley, CA 94720-1460, USA.

SSDI 0022-328X(94)05336-7

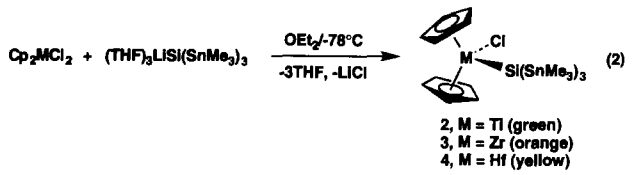

procedure provides somewhat lower yields of **2**, for which shorter reaction times and lower temperatures are optimal. The interesting way in which the colors of these pentane-soluble compounds vary according to the nature of the metal center suggests the presence of silyl ligand-to-metal charge transfer transitions [10]. The successful isolation of **2** is notable, because very few d^0 titanocene silyl derivatives are known [1]. Whereas $Cp_2Ti(SiMe_3)$-Cl has been reported [11], $Cp_2Ti[Si(SiMe_3)_3]Cl$ could not be isolated from reactions of Cp_2TiCl_2 with $(THF)_3LiSi(SiMe_3)_3$ [12]. The slow thermal decomposition of **2** prevents room-temperature storage of the compound.

The spectroscopic properties for **3** and **4** are similar to those observed for the analogous $Cp_2M[Si(SiMe_3)_3]Cl$ (M = Zr, Hf) complexes. The difference in $^1J_{SiSn}$ coupling constants between **4** (131 Hz) and **3** (120 Hz) is consistent with the periodic trend previously observed for the Group 6 complexes $[NEt_4][(CO)_5MSi(SnMe_3)_3]$ (M = Cr, Mo, W) [8].

3. Structural studies

The molecular structures of **1** and **3** are depicted in Figs. 1 and 2, and relevant geometrical parameters are listed in Tables 1–4. Both compounds adopt bent-metallocene, pseudo-tetrahedral geometries. The asymmetric unit in the structure of **3** contains two independent

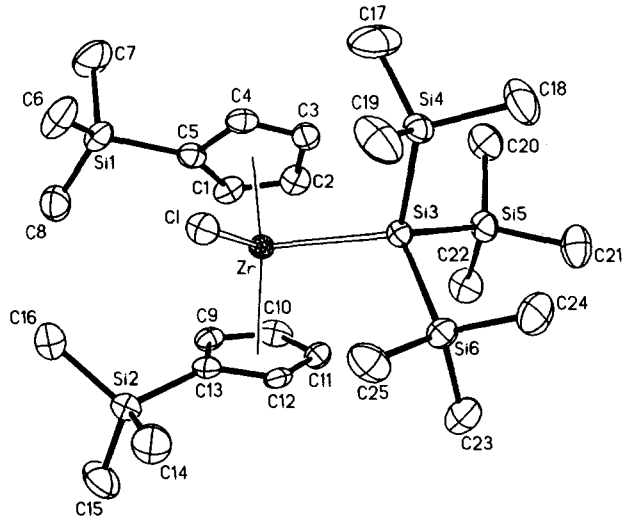

Fig. 1. ORTEP diagram of $(\eta^5\text{-}C_5H_4SiMe_3)_2Zr[Si(SiMe_3)_3]Cl$ (**1**).

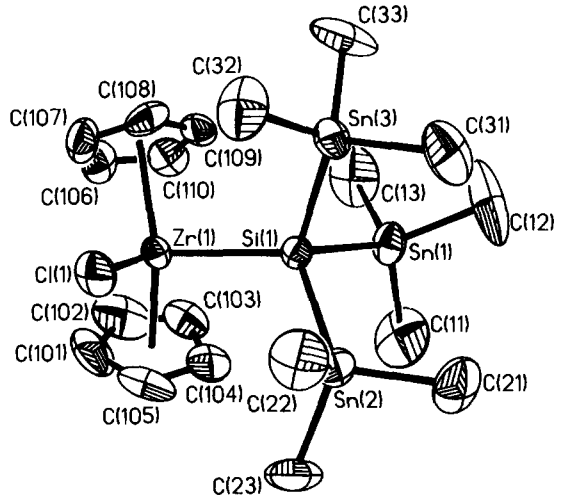

Fig. 2. ORTEP diagram of $Cp_2Zr[Si(SnMe_3)_3]Cl$ (**3**).

molecules. The Zr–C_5 ring centroid distances are nearly identical for **1** and **3** (2.21 (1) Å and 2.19 (1) Å, respectively), and the centroid–Zr–centroid angles are

Table 1
Atomic coordinates ($\times 10^4$) and equivalent isotropic displacement coefficients ($Å^2 \times 10^3$) for $(\eta^5\text{-}C_5H_4SiMe_3)_2Zr[Si(SiMe_3)_3]Cl$ (**1**)

Atom	x	y	z	U_{eq} [a]
Zr	5419.3(7)	5869.9(5)	2611.9(4)	35.4(3)
Cl	4994(2)	7390(1)	2480(1)	53(1)
Si(1)	2572(2)	5841(2)	1017(2)	60(1)
Si(2)	3759(2)	6741(2)	3945(2)	56(1)
Si(3)	7676(2)	6198(2)	2868(1)	39(1)
Si(4)	8041(2)	7160(2)	2021(2)	49(1)
Si(5)	8797(2)	4984(2)	2883(2)	54(1)
Si(6)	8536(2)	6913(2)	3969(2)	53(1)
C(1)	4423(8)	4723(6)	1768(5)	50(4)
C(2)	5526(9)	4628(6)	1833(5)	56(5)
C(3)	5863(8)	5345(6)	1512(5)	52(4)
C(4)	4947(8)	5875(7)	1267(4)	53(4)
C(5)	4031(8)	5508(6)	1419(5)	49(4)
C(6)	2451(10)	7024(7)	964(6)	96(6)
C(7)	2141(10)	5389(8)	84(6)	107(6)
C(8)	1697(9)	5380(8)	1530(6)	88(6)
C(9)	4419(8)	5148(6)	3362(5)	47(4)
C(10)	5371(10)	4662(6)	3432(5)	58(5)
C(11)	6257(8)	5162(6)	3809(5)	51(4)
C(12)	5860(7)	5954(6)	3976(4)	41(4)
C(13)	4702(7)	5955(6)	3703(4)	43(4)
C(14)	4574(9)	7675(7)	4395(6)	87(6)
C(15)	3197(10)	6144(8)	4587(6)	99(7)
C(16)	2622(8)	7088(7)	3157(6)	77(5)
C(17)	7266(12)	7003(10)	1069(6)	132(8)
C(18)	9512(9)	7161(8)	2031(7)	98(7)
C(19)	7718(11)	8275(7)	2208(7)	108(7)
C(20)	8676(9)	4584(7)	1949(6)	83(6)
C(21)	10282(8)	5190(7)	3336(6)	84(6)
C(22)	8421(9)	4054(6)	3376(5)	72(5)
C(23)	8822(9)	6192(7)	4774(6)	85(5)
C(24)	9910(8)	7381(8)	4020(6)	89(6)
C(25)	7697(9)	7838(6)	4124(6)	79(6)

[a] Equivalent isotropic U defined as one third of the trace of the orthogonalized U_{ij} tensor.

Table 2
Atomic coordinates ($\times 10^4$) and equivalent isotropic displacement coefficients ($Å^2 \times 10^3$) for $Cp_2Zr[Si(SnMe_3)_3]Cl$ (3)

Atom	x	y	z	U_{eq} [a]
Zr(1)	−1384(1)	3351(1)	7946(1)	58(1)
Zr(2)	1052(1)	1650(1)	2056(1)	58(1)
Si(1)	794(3)	3246(2)	7518(2)	57(1)
Si(2)	3630(3)	1788(2)	2511(2)	56(1)
Sn(1)	1382(1)	1754(1)	7042(1)	89(1)
Sn(2)	2758(1)	4107(1)	8670(1)	87(1)
Sn(3)	814(1)	3876(1)	6290(1)	75(1)
Sn(4)	4524(1)	1175(1)	1311(1)	93(1)
Sn(5)	4838(1)	3271(1)	3174(1)	92(1)
Sn(6)	4707(1)	951(1)	3558(1)	95(1)
Cl(1)	−1086(4)	4881(2)	8400(3)	95(2)
Cl(2)	767(5)	117(2)	1616(3)	98(2)
C(11)	2192(29)	1239(16)	8088(18)	207(22)
C(12)	2590(29)	1691(15)	6293(20)	223(26)
C(13)	−261(24)	832(11)	6273(15)	172(16)
C(21)	4443(17)	3708(14)	8484(14)	156(12)
C(22)	2841(21)	5421(11)	8690(14)	145(13)
C(23)	2982(20)	4086(15)	9946(10)	140(12)
C(31)	2678(20)	4051(14)	6178(14)	147(14)
C(32)	51(21)	5069(12)	6366(15)	142(14)
C(33)	−300(22)	3035(16)	5061(9)	164(13)
C(41)	6452(18)	1026(18)	1710(16)	175(16)
C(42)	3471(33)	−78(21)	577(22)	345(31)
C(43)	4546(31)	1988(22)	493(17)	241(28)
C(51)	4182(28)	4185(15)	2542(24)	304(28)
C(52)	6689(21)	3325(16)	3302(26)	298(29)
C(53)	4974(55)	3805(27)	4452(28)	520(59)
C(61)	4336(30)	−381(15)	2873(25)	355(31)
C(62)	6636(18)	1124(13)	4005(14)	140(12)
C(63)	4235(30)	1144(35)	4684(20)	371(46)
C(101)	−1650(33)	3310(23)	9303(16)	148(17)
C(102)	−2012(32)	2516(23)	8801(17)	159(19)
C(103)	−1101(28)	2175(13)	8610(13)	109(11)
C(104)	4(23)	2726(16)	9042(13)	112(11)
C(105)	−375(30)	3474(13)	9470(10)	125(12)
C(106)	−3560(15)	2720(13)	7051(11)	100(9)
C(107)	−3388(16)	3500(14)	6924(12)	111(10)
C(108)	−2491(14)	3492(13)	6505(10)	96(8)
C(109)	−2129(15)	2694(12)	6390(9)	88(7)
C(110)	−2758(16)	2224(11)	6745(10)	94(8)
C(201)	−487(21)	2241(22)	1030(17)	144(15)
C(202)	−106(28)	1509(14)	540(11)	119(11)
C(203)	1037(25)	1648(16)	582(12)	111(12)
C(204)	1512(19)	2421(15)	1065(12)	104(10)
C(205)	623(28)	2818(12)	1375(13)	117(11)
C(206)	−161(27)	2360(20)	2920(15)	143(15)
C(207)	1031(25)	2768(12)	3305(12)	113(11)
C(208)	1787(17)	2238(12)	3652(9)	92(8)
C(209)	1127(17)	1471(12)	3468(11)	90(9)
C(210)	−69(20)	1565(16)	3042(12)	115(11)

[a] Equivalent isotropic U defined as one third of the trace of the orthogonalized U_{ij} tensor.

also nearly the same (128.3 (4)° and 130.4 (2)°, respectively). For complex **1**, the sterically demanding $-Si(SiMe_3)_3$ group results in an eclipsed-like geometry for the η^5-$C_5H_4SiMe_3$ ligands, and relatively close contact between the two $-SiMe_3$ substituents. A somewhat similar geometry was reported for $(\eta^5$-$C_5H_4SiMe_3)_2Zr[CH(SiMe_3)_2]Cl$ [13]. As expected, the metrical data are consistent with more crowding via interligand repulsions for **1** (vs. **3**). Thus, the average Zr–C(Cp) distances in **1** (2.51 Å and 2.52 Å) are somewhat greater than the corresponding values for **3** (2.48 Å and 2.49 Å). However the crowding in **1** appears to be slightly less than that in $(\eta^5$-$C_5H_4SiMe_3)_2Zr[CH(SiMe_3)_2]Cl$, which has Zr–C(Cp) distances which average to 2.54 Å [13].

The Zr–Si distance of 2.833 (3) Å for **1** is remarkably similar to the previously determined Zi–Si bond lengths in $Cp_2Zr(SiPh_3)Cl$ (2.813 (2) Å) [14] and $Cp_2Zr(SiMe_3)S_2CNEt_2$ (2.815 (1) Å) [15]. The slightly shorter Zr–Si distance in **3**, which averages to 2.768 (4) Å, probably reflects less steric crowding in that complex. In this regard, note that the Si–Sn distances in the $-Si(SnMe_3)_3$ group (average 2.57 Å) are longer than the Si–Si distances in **1** (average 2.38 Å), and the Sn–Si–Sn bond angles of **3** (average 102.3°) are on average slightly more acute than the Si–Si–Si angles of **1** (103.7°). In general, the geometric parameters for the $-Si(SnMe_3)_3$ ligand closely resemble those observed in $[NEt_4][(CO)_5WSi(SnMe_3)_3]$ [8].

4. Reactivity studies

Initial reactivity studies with the new silyl complexes **1–4** have focused on transformations involving the M–Cl and M–Si bonds. The reaction of **1** with MeMgCl in diethyl ether gave the expected methyl derivative $(\eta^5$-$C_5H_4SiMe_3)_2Zr[Si(SiMe_3)_3]Me$ (**5**) as orange crystals, but this compound has so far not been successfully separated, via fractional crystallization, from small quantities of unreacted **1**. Compound **5** is therefore identified solely on the basis of its ^1H NMR spectrum, which contained (in addition to the expected trimethyl silyl peaks), a resonance for the methyl ligand at δ

Table 3
Selected bond distances (Å) and angles (Deg) for $(\eta^5$-$C_5H_4SiMe_3)_2Zr[Si(SiMe_3)_3]Cl$ (**1**) [a]

Bond distances			
Zr–CNT (av)	2.21(1)	C(13)–Si(2)	1.879(10)
Zr–Si(3)	2.833(3)	Si(3)–Si(4)	2.378(4)
Zr–Cl	2.430(2)	Si(3)–Si(5)	2.373(5)
C(5)–Si(1)	1.873(9)	Si(3)–Si(6)	2.376(4)
Bond angles			
CNT(1)–Zr–CNT(2)	128.3(4)	Zr–Si(3)–Si(4)	113.3(1)
CNT(1)–Zr–Cl	111.3(2)	Zr–Si(3)–Si(5)	116.2(1)
CNT(2)–Zr–Cl	111.4(2)	Zr–Si(3)–Si(6)	114.7(1)
CNT(1)–Zr–Si(3)	102.9(2)	Si(4)–Si(3)–Si(5)	105.6(2)
CNT(2)–Zr–Si(3)	103.7(2)	Si(4)–Si(3)–Si(6)	101.2(1)
Cl–Zr–Si(3)	91.5(1)	Si(5)–Si(3)–Si(6)	104.3(1)

[a] CNT is the centroid for the η^5-$C_5H_4SiMe_3$ rings.

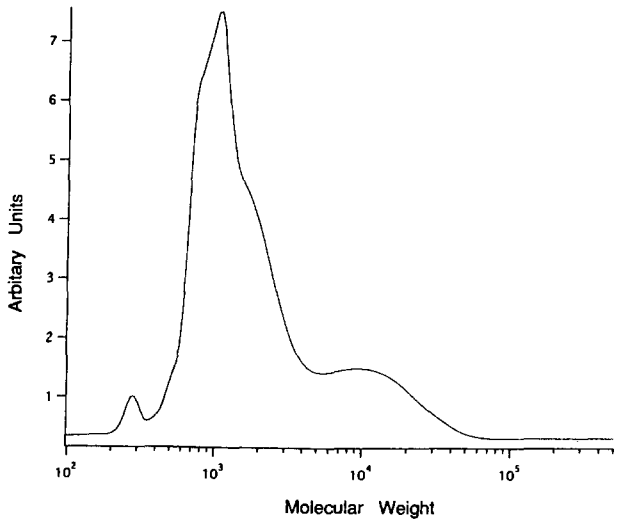

Fig. 3. Gel permeation chromatogram for the dehydropolymerization of neat $^{n}Bu_2SnH_2$ by **1** (polystyrene standards).

-0.21, and four cyclopentadienyl hydrogens at δ 5.66, 5.75, 6.84, and 7.47.

Part of the motivation for examining silyl complexes with various cyclopentadienyl derivatives as ligands stems from the strong influence that cyclopentadienyl substitutions may have on the behavior of Group 4 metallocene complexes as catalysts for the dehydropolymerization of hydrosilanes. For example, we have found that $Cp(\eta^5\text{-}C_5Me_5)Zr$ derivatives are much more active toward elongation of $H(SiHPh)_nH$ chains than analogous Cp_2Zr complexes [6,7]. Because it seemed that the $(\eta^5\text{-}C_5H_4SiMe_3)_2Zr$ fragment might be *sterically* similar to $Cp(\eta^5\text{-}C_5Me_5)Zr$ (vs. Cp_2Zr), it was of interest to examine the catalytic behavior of **1** and related derivatives.

Addition of neat $PhSiH_3$ to **1** resulted in a wine-red mixture, but no hydrogen evolution as is typically observed for the more active catalysts. After about 10 min, some hydrogen evolution was observed as the mixture became viscous. However, after 24 h, the reaction mixture had not yet solidified and analysis by gel permeation chromatography (gpc; polystyrene standards) revealed a bimodal molecular weight distribution corresponding to a mixture of oligomeric $(SiHPh)_n$ cyclics ($n \approx 5$–6, 13%) and linear $H(SiHPh)_mH$ chains (M_w/M_n = 1810/900). By comparison, $Cp(\eta^5\text{-}C_5Me_5)Zr[Si(SiMe_3)_3]Cl$ produces after 24 h a mixture of cyclics (15%) and linear polysilanes with M_w/M_n = 3280/1870 [7]. Based on this result it appears that in general, $Cp(\eta^5\text{-}C_5Me_5)Zr$ derivatives are more effective as catalysts for the dehydropolymerization of $PhSiH_3$. This conclusion is further supported by recent results obtained for other Group 4 catalysts containing $(\eta^5\text{-}C_5H_4SiMe_3)$ ligands [7].

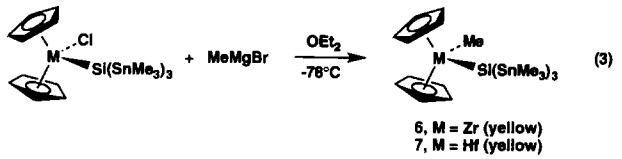

The dehydropolymerization of $^{n}Bu_2SnH_2$ by **1** affords polystannanes with a broad molecular weight distribution (M_w/M_n = 4800/1420). Thus **1** is not very active toward the dehydrocoupling of $^{n}Bu_2SnH_2$, compared to many other zirconocene catalysts [16,17]. Examination of the gpc trace (Fig. 3) reveals that the sample is dominated by a relatively low molecular weight mode at ca. 1100 amu. However, a small amount of higher polymer gives rise to a band centered at ca. 10,000 amu. Overall this molecular weight distribution profile is unusual for polymerizations with $^{n}Bu_2SnH_2$ monomer [17], for reasons that are not presently evident.

Reactions of **3** and **4** with MeMgBr give isolable methyl derivatives, as shown in Eq. 3. Compounds **6** and **7** are analogous to the previously reported $Cp_2M[Si(SiMe_3)_3]Me$ derivatives [2,18].

Compounds **3** and **4** do not undergo insertion reactions with carbon monoxide, even at higher pressures (5–7 atm). In this regard, these compounds are similar to analogous–$Si(SiMe_3)_3$ derivatives, but unlike most 16-electron zirconocene and hafnocene silyl complexes,

Table 4
Selected bond distances (Å) and angles (Deg) for $Cp_2Zr[Si(SnMe_3)_3]Cl$ (**3**) [a,b]

Bond distances			
Zr(1)–CNT (av)	2.19(1)	Si(1)–Sn(1)	2.563(4), 2.570(4)
Zr(1)–Si(1)	2.772(4), 2.765(4)	Si(1)–Sn(2)	2.570(4), 2.559(3)
Zr(1)–Cl(1)	2.417(4), 2.421(4)	Si(1)–Sn(3)	2.576(4), 2.575(4)
Bond angles			
CNT–Zr(1)–CNT (av)	130.4(2)	Zr(1)–Si(1)–Sn(3)	114.9(1), 115.7(2)
Cl(1)–Zr(1)–Si(1)	93.6(2), 94.9(1)	Sn(1)–Si(1)–Sn(2)	106.0(1), 102.8(1)
Zr(1)–Si(1)–Sn(1)	116.4(1), 115.6(1)	Sn(1)–Si(1)–Sn(3)	102.5(1), 99.2(1)
Zr(1)–Si(1)–Sn(2)	115.0(1), 117.8(1)	Sn(2)–Si(1)–Sn(3)	100.0(1), 103.2(1)

[a] CNT is the centroid for the Cp rings.
[b] Where appropriate, parameters for both independent molecules are listed.

which readily react with carbon monoxide to give η^2-silaacyl compounds [1–4]. Interestingly, the titanium analog **2** reacts with carbon monoxide (1–6 atm) via reductive elimination to $Cp_2Ti(CO)_2$ and $ClSi(SnMe_3)_3$ [8] (Eq. 4, by ^1H NMR spectroscopy).

The titanium silyl $Cp_2Ti(SiMe_3)Cl$ also eliminates silyl chloride upon exposure to carbon monoxide [2]. The reaction of **2** with one equivalent of $PhSiH_3$ in benzene-d_6 quantitatively produces a 2:1 mixture of the σ-bond metathesis product $HSi(SnMe_3)_3$ [8] and the reductive elimination product $ClSi(SnMe_3)_3$. The titanium-containing products in this reaction could not be identified (the presumed kinetic products are $Cp_2Ti(SiH_2Ph)Cl$ and $Cp_2Ti(SiH_2Ph)H$).

5. Experimental details

All manipulations employed strictly anhydrous and anaerobic conditions, with use of Schlenk techniques or a Vacuum Atmospheres glove box. Elemental analyses were performed by Schwartzkopf Microanalytical Laboratory, Mikroanalytisches Labor Pascher, or Desert Analytical Laboratory. IR spectra were recorded on a Perkin-Elmer 1330 spectrometer. NMR spectra were recorded with a GE-QE 300 instrument. The compounds $(\eta^5\text{-}C_5H_4SiMe_3)_2ZrCl_2$ [9], $(THF)_3LiSi(SiMe_3)_3$ [19] and $(THF)_3LiSi(SnMe_3)_3$ [8] were prepared according to published procedures. The reaction of $Cp_2Ti[Si(SnMe_3)_3]Cl$ with carbon monoxide was monitored by ^1H NMR and IR spectroscopy.

5.1. $(\eta^5\text{-}C_5H_4SiMe_3)_2Zr[Si(SiMe_3)_3]Cl$ (1)

The complex $(\eta^5\text{-}C_5H_4SiMe_3)_2ZrCl_2$ (0.40 g, 0.91 mmol), $Li(THF)_{2.5}LiSi(SiMe_3)_3$ (0.56 g, 1.26 mmol), and 70 ml of diethyl ether were added to a 250 ml Schlenk flask at room temperature. The resulting dark-red solution was stirred for 10 h, and then the volatile material was removed by vacuum transfer. The product was extracted into 100 ml of pentane, and crystallized from this solvent via concentration and cooling (−43°C) of the extract. Total yield 34% (0.20 g). Anal. Calc. for $C_{25}H_{53}ClSi_6Zr$: C, 46.3; H, 8.23. Found: C, 46.2; H, 8.24%. ^1H NMR (benzene-d_6, 300 MHz, 23°C): δ 0.25 (s, 18 H, $C_5H_4SiMe_3$), 0.47 (s, 27 H, $Si(SiMe_3)_3$), 5.01, 5.81, 6.75, 7.66 (m, 4 H, $C_5H_4SiMe_3$). $^{13}C\{^1H\}$ NMR (benzene-d_6, 75.5 Hz, 23°C): δ 0.12 ($C_5H_4SiMe_3$), 5.16 ($Si(SiMe_3)_3$), 111.50, 112.40, 114.79, 120.39, 129.41 ($C_5H_4SiMe_3$). IR (Nujol, CsI, cm^{-1}): 1257 m, 1238 m, 1168 w, 1150 w, 1050 w, 1021 m, 940 w, 858 sh s, 832 s, 795 s, 720 m, 680 m, 619 m, 598 m, 398 w, 356 m, 332 m, 300 w.

5.2. $Cp_2Ti[Si(SnMe_3)_3]Cl$ (2)

The procedure was analogous to that for **3**, starting with Cp_2TiCl_2 (0.13 g, 0.51 mmol), $(THF)_3LiSi(SnMe_3)_3$ (0.37 g, 0.50 mmol), and Et_2O (25 ml). After warming to room temperature, the reaction mixture was stirred for 1 h, and then the volatile material was removed from the dark-green reaction mixture. Two crops of dark-green crystals were obtained from pentane, in a combined yield of 0.081 g (0.11 mmol, 22%). Acceptable combustion analyses were precluded by the thermal instability of the compound. ^1H NMR (benzene-d_6, 300 MHz, 23°C): δ 0.40 (s, $^2J_{SnH}$ = 44.4 Hz, 27 H, $SnMe_3$), 5.90 (s, 10 H, Cp). $^{13}C\{^1H\}$ NMR (benzene-d_6, 75.5 Hz, 23°C): δ-5.08 ($^1J_{SnC}$ = 216.1, 226.0 Hz, $^3J_{SnC}$ = 11.6 Hz, $SnMe_3$), 114.8 (Cp).

5.3. $Cp_2Zr[Si(SnMe_3)_3]Cl$ (3)

Cp_2ZrCl_2 (1.22 g, 4.18 mmol) and $(THF)_3LiSi(SnMe_3)_3$ (3.10 g, 4.18 mmol) were placed in a 100 ml flask. The combined solids were cooled to −78°C, and then Et_2O (60 ml) was added. After the resulting heterogeneous orange mixture was stirred for 15 min, the cold bath was removed and the reaction mixture gradually warmed to room temperature. The reaction darkened to a red-orange heterogeneous mixture during stirring over 18 h. The volatile materials were removed in vacuo. The resulting dark orange-red residue was extracted with pentane (2 × 40 ml, 1 × 20 ml). Cooling the orange solution to −35°C gave an initial crop of 2.18 g (2.81 mmol) of orange crystals. A second crop of 0.33 g (0.43 mmol) of orange crystals produced a total yield of 77.5%. Anal. Calc. for $C_{19}H_{37}ClSiSn_3Zr$: C, 29.4; H, 4.80; Cl, 4.57. Found: C, 29.3; H, 4.59; Cl, 4.49%. Mp: > 152°C (dec). ^1H NMR (benzene-d_6, 300 MHz, 23°C): δ 0.42 (s, $^2J_{SnH}$ = 44.1 Hz, 27 H, $SnMe_3$), 5.90 (s, 10 H, Cp). $^{13}C\{^1H\}$ NMR (benzene-d_6, 75.5 Hz, 23°C): δ-5.15 ($^1J_{SnC}$ = 219.4, 229.5 Hz, $^3J_{SnC}$ = 11.8 Hz, $SnMe_3$), 111.9 (Cp). $^{29}Si\{^1H\}$ NMR (benzene-d_6, 59.6 MHz, 23°C): δ 1.88 ($^1J_{SiSn}$ = 119.6 Hz). IR (Nujol, CsI, cm^{-1}): 3002 w, 1261 w, 1177 m, 1171 m sh, 1066 w, 1018 s, 835 m, 809 vs, 757 br vs, 503 s, 348 m, 289 w.

5.4. $Cp_2Hf[Si(SnMe_3)_3]Cl$ (4)

The synthesis was analogous to that for **3**, starting with Cp_2HfCl_2 (1.91 g, 5.03 mmol) and $(THF)_3LiSi(SnMe_3)_3$ (3.74 g, 5.04 mmol). The total yield of yellow

crystals was 3.58 g (4.15 mmol, 82.5%). Anal. Calc. for $C_{19}H_{37}ClHfSiSn_3$: C, 26.4; H, 4.32; Cl, 4.10. Found: C, 26.6; H, 4.40; Cl, 4.05%. Mp: > 185°C (dec). ^{1}H NMR (benzene-d_6, 300 MHz, 23°C): δ 0.40 (s, $^2J_{SnH}$ = 44.3 Hz, 27 H, $SnMe_3$), 5.82 (s, 10 H, Cp). $^{13}C\{^1H\}$NMR (benzene-d_6, 75.5 Hz, 23°C): δ-5.01 ($^1J_{SnC}$ = 218.5, 228.6 Hz, $^3J_{SnC}$ = 12.3 Hz, $SnMe_3$), 111.0 (Cp). $^{29}Si\{^1H\}$ NMR (benzene-d_6, 59.6 MHz, 23°C): δ7.61 ($^1J_{SiSn}$ = 130.7 Hz). IR (Nujol, CsI, cm^{-1}): 3106 w, 1261 w, 1178 m, 1174 m sh, 1127 w, 1067 w, 1019 s, 840 m, 813 vs. 758 br vs, 503 s, 350 br w, 316 m, 302 w sh.

5.5. $(\eta^5$-$C_5H_4SiMe_3)_2Zr[Si(SiMe_3)_3]Me$ (5)

Complex **1** (0.43 g, 0.66 mmol) was dissolved in diethyl ether (50 ml), and the resulting solution was cooled to −78°C. After addition of 3.0 M MeMgCl (0.22 ml, 0.65 mol) via syringe, the reaction solution was allowed to warm to room temperature. Stirring for 10 h at room temperature resulted in an orange suspension. Removal of volatile material by vacuum transfer, extraction of the resulting residue with pentane, and concentration and cooling (−43°C) of the pentane extract afforded orange needles. These crystals were contaminated with unreacted **1** (1–10%). ^{1}H NMR (benzene-d_6, 300 MHz, 23°C): δ −0.21 (s, 3 H, ZrMe), 0.15 (s, 18 H, $C_5H_4SiMe_3$), 0.44 (s, 27 H, $Si(SiMe_3)_3$), 5.66, 5.75, 6.84, 7.47 (m, 4 H, $C_5H_4SiMe_3$).

5.6. Polymerizations

In each case, 0.30 g of the monomer was added to the catalyst (1 mol% of **1**) in the inert-atmosphere glove box. The reaction vessel was then transferred to a vacuum line, and vented to an atmosphere of nitrogen. The molecular weights (vs. polystyrene standards) were determined with a Waters Associates Chromatograph equipped with a refractive index detector and 500 Å, 10^3 Å, and 10^4 Å Ultrastyragel columns in series (tetrahydrofuran solvent).

5.7. $Cp_2Zr[Si(SnMe_3)_3]Me$ (6)

The preparation of this compound was analogous to that for **7** below, starting with $Cp_2Zr[Si(SnMe_3)_3]Cl$ (0.89 g, 1.2 mmol), a 0.45 M solution of MeMgBr (2.6 ml, 1.2 mmol), and pentane (30 ml). Dark-yellow crystals were obtained from a cooled solution of pentane, providing 0.49 g (56%) of product. Attempts to obtain combustion analyses appeared to fail because of slow thermal decomposition of the compound. ^{1}H NMR (benzene-d_6, 300 MHz, 23°C): δ-0.26 (s, $^4J_{SnH}$ = 3.6 Hz, 3 H, ZrMe, 0.38 (s, $^2J_{SnH}$ = 43.5 Hz, 27 H, $SnMe_3$), 5.87 (s, 10 H, Cp).

5.8. $Cp_2Hf[Si(SnMe_3)_3]Me$ (7)

A flask was charged with $Cp_2Hf[Si(SnMe_3)_3]Cl$ (0.64 g, 0.74 mmol) and Et_2O (30 ml) and cooled to −78°C. A 2.8 M solution of MeMgBr in Et_2O (0.27 ml, 0.76 mmol) was then added to the yellow solution. After stirring for 20 min, the cold bath was removed, allowing the murky yellow solution to gradually warm to room temperature. The now heterogeneous yellow mixture was subsequently stirred at room temperature for 1.5 h. The volatiles were removed in vacuo, and the light yellow residue was extracted with pentane (1 × 30 ml, 1 × 10 ml). After filtration removed the white insolubles, the yellow pentane solution was concentrated to 10 ml and placed at −35°C. Two crops of light-yellow crystals were obtained, totalling 0.35 g (57%). Mp: > 165°C (dec). ^{1}H NMR (benzene-d_6, 300 MHz, 23°C): δ −0.56 (s, $^4J_{SnH}$ = 4.2 Hz, 3 H, HfMe), 0.38 (s, $^2J_{SnH}$ = 43.5 Hz, 27 H, $SnMe_3$), 5.78 (s, 10 H, Cp). $^{13}C\{^1H\}$ NMR (benzene-d_6, 75.5 Hz, 23°C): δ −4.94 ($^1J_{SnC}$ = 215.6, 225.7 Hz, $^3J_{SnC}$ = 13.2 Hz, $SnMe_3$), 51.2 (HfMe), 109.6 (Cp). EI-HRMS: Found m/z (M^+) 847.944. Calc.: 847.943. IR (Nujol, CsI, cm^{-1}): 1259 w, 1179 w, 1146 w, 1075 w, 1017 m, 808 s, 755 br s, 504 m, 493 m sh.

5.9. X-ray structure determination of $(\eta^5$-$C_5H_4SiMe_3)_2Zr[Si(SiMe_3)_3]Cl$ (1)

Crystallographic data are collected in Table 5. Crystals were mounted in glass capillaries and found to

Table 5
Crystallographic data for compounds **1** and **3**

Chemical formula	$C_{25}H_{53}ClSi_6Zr$ (1)	$C_{19}H_{37}ClSiSn_3Zr$ (3)
a (Å)	12.829(3)	11.300(3)
b (Å)	15.603(2)	16.401(4)
c (Å)	19.481(5)	17.212(5)
α, deg	–	104.15(2)
β, deg	107.43(2)	101.00(2)
γ, deg	–	92.12(2)
V (Å^3)	3720.5(12)	2929.4(13)
Z	4	4
$\rho_{calc.}$ (g cm^{-3})	1.158	1.760
μ (Mo Kα) (cm^{-1})	5.65	30.16
Formula weight	648.9	776.3
Space group	$P2_1/c$	$P\bar{1}$
Diffractometer	Siemens P4	Nicolet R3m/V
Radiation	Mo Kα	Mo Kα
λ (Å)	0.71073	0.71073
T (K)	296	297
2θ range, deg	4–45	3–48
Reflections collected	7594	10829
Independent reflections	4727	9241
Observed reflections	2502 ($5\sigma F$)	5690 ($6\sigma F$)
$R(F)$, $R(wF)$, %	4.67, 5.47	6.16, 8.34
GOF	0.99	1.58
Δ/σ (max)	0.001	0.003
N_o/N_v	8.4	12.6
$\Delta\rho$, e Å^{-3}	0.38	1.62

possess $2/m$ Laue symmetry. Systematic absences in the diffraction data were uniquely consistent with the space group $P2_1/c$. Variations in azimuthal scan data of less than 10% indicated that corrections for absorption were unnecessary. The Zr atom was located from a Patterson map. All non-hydrogen atoms were refined anisotropically, and hydrogen atoms were idealized using a riding model. All computations used SHELXTL-PC (ver. 4.2, G.M. Sheldrick, Siemens XRD, Madison, WI).

5.10. X-ray structure determination of $Cp_2Zr[Si(SnMe_3)_3]Cl$ (3)

Crystallographic data are collected in Table 5. An irregularly shaped orange crystal was mounted under nitrogen in a glass-walled capillary. Centering of 25 randomly selected reflections with $15° \leq 2\theta \leq 30°$ provided the unit cell dimensions. Data were corrected for crystal decay (11%), Lorentz and polarization effects, and absorption. Despite the presence of a systematic absence indicting a 2_1(b) screw axis, no higher symmetry Bravais lattices could be fitted to the unit cell parameters. The Zr atoms were located by direct methods, and all remaining non-hydrogen atoms were located and refined anisotropically by difference Fourier and full-matrix least-squares methods (SHELXTL PLUS computer programs, Siemens Instrument Corp., Madison, WI). Hydrogen atoms were fixed in calculated, idealized positions (d(C–H) = 0.96 Å, fixed isotropic thermal parameters 1.2 times the isotropic thermal parameter for the carbon to which it is attached).

5.11. Supplementary material available

Full crystallographic data including structure factor tables may be obtained from one of the authors (TDT).

Acknowledgement

We thank the Divisions of Chemistry and Materials Research at the National Science Foundation and Japan Energy Co., Ltd. for support of this work.

References

[1] T.D. Tilley, in S. Patai and Z. Rappoport (eds.), *The Silicon-Heteroatom Bond*, Wiley, New York, 1991, Chs. 9 and 10.
[2] B.K. Campion, J. Falk and T.D. Tilley, *J. Am. Chem. Soc., 109* (1987) 2049.
[3] F.H. Elsner, T.D. Tilley, A.L. Rheingold and S.J. Geib, *J. Organomet. Chem., 358* (1988) 169.
[4] D.M. Roddick, R.H. Heyn and T.D. Tilley, *Organometallics, 8* (1989) 324.
[5] J.F. Harrod, Y. Mu and E. Samuel, *Polyhedron, 10* (1991) 1239.
[6] T.D. Tilley, *Acc. Chem. Res., 26* (1993) 22.
[7] T. Imori and T.D. Tilley, *Polyhedron 13* (1994) 2231.
[8] R.H. Heyn and T.D. Tilley, *Inorg. Chem., 29* (1990) 4051.
[9] M.F. Lappert, C.J. Pickett, P.I. Riley and P.I.W. Yarrow, *J. Chem. Soc., Dalton Trans.*, (1981) 805.
[10] H.-G. Woo, R.H. Heyn and T.D. Tilley, *J. Am. Chem. Soc., 114* (1992) 5698.
[11] L. Rösch, G. Altnau, W. Erb, J. Pickhardt and N. Bruncks, *J. Organomet. Chem., 197* (1980) 51.
[12] B.K. Campion and T.D. Tilley, unpublished results.
[13] M.F. Lappert, P.I. Riley, P.I.W. Yarrow, J.L. Atwood, W.E. Hunter and M.J. Zaworotko, *J. Chem. Soc., Dalton Trans.*, (1981) 814.
[14] K.W. Muir, *J. Chem. Soc., A* (1971) 2663.
[15] T.D. Tilley, *Organometallics, 4* (1985) 1452.
[16] T. Imori and T.D. Tilley, *J. Chem. Soc., Chem. Commun.*, (1993) 1607.
[17] T. Imori, V. Lu, H. Cai and T.D. Tilley, in preparation.
[18] H.-G. Woo, J.F. Walzer and T.D. Tilley, *J. Am. Chem. Soc., 114* (1992) 7047.
[19] G. Gutekunst and A.G. Brook, *J. Organomet. Chem.*, 225 (1982) 1.